Journal of the Taiwan Institute of Chemical Engineers 45 (2014) 3085–3089

Contents lists available at ScienceDirect

Journal of the Taiwan Institute of Chemical Engineers

journal homepage: www.elsevier.com/locate/jtice

Surface-enhanced infrared absorption spectra of eicosanoic acid on confeito-like Au nanoparticle

Masaki Ujihara [a,*], Nhut Minh Dang [b], Chia-Chi Chang [b], Toyoko Imae [a,b]

[a] Graduate Institute of Applied Science and Technology, National Taiwan University of Science and Technology, 43 Keelung Road, Section 4, Taipei 10607, Taiwan

[b] Department of Chemical Engineering, National Taiwan University of Science and Technology, 43 Keelung Road, Section 4, Taipei 10607, Taiwan

ARTICLE INFO

Article history:
Received 17 February 2014
Received in revised form 23 June 2014
Accepted 24 June 2014
Available online 17 July 2014

Keywords:
Gold nanoparticle
Confeito-like nanoparticle
Surface-enhanced infrared absorption spectroscopy
Surface plasmon
Eicosanoic acid

ABSTRACT

Surface-enhanced infrared absorption spectra of eicosanoic acid were measured with transmission mode using citrate-protected confeito-like Au nanoparticles on a CaF_2 substrate. The absorption bands of the alkyl chain in eicosanoic acid were significantly enhanced around 200-fold of the control. This enhancing effect decreased, when the Au nanoparticles were dialyzed to remove excess citrate, suggesting that the citrate covering the Au nanoparticles played the role of anchoring the eicosanoic acid on the Au nanoparticles. It was also confirmed that the eicosanoic acid on the Au nanoparticles with the citrate was more ordered than that on the Au nanoparticles without the coverage of citrate. These findings are useful to design the plasmonics devices with ultrasensitive assay using the surface-enhanced infrared absorption spectroscopy based on the simple procedure.

1. Introduction

Metallic surfaces have unique optical properties due to the collective oscillations of their free electrons [1–3]. The oscillations are called surface plasmon, and their properties reflect several factors such as dielectric constants of the metal and the surrounding medium [1–4]. When the metallic materials have nano-structures, their structures strongly affect the oscillation states as the localization of the surface plasmon [1–5]. Typically, a dispersion of Au nanoparticles (AuNPs) with spherical shapes indicates red color and has an absorption band in a range of 520–580 nm depending on their size, which is caused by the resonance of light with the localized surface plasmon [2,6,7].

When the localized surface plasmon resonates with the incident light, a strong electric field is formed in the vicinity of the particle [1–5]. This electric field can intensify the optical response of materials near the particle, *e.g.* Raman scattering [8,9] and infrared (IR) absorption [10,11]. Then, the AuNPs can be used for spectroscopies with ultrahigh sensitivity [12]. Today, the surface-enhanced Raman scattering (SERS) is widely examined for ultrasensitive analysis [8,9,13]. The surface-enhanced IR absorption spectroscopy (SEIRAS) is also applicable for such sensing; however the reports are rather minor despite the popularity of Fourier transform (FT)-IR spectrophotometer [11,14–18]. While the Raman scattering can be intensified million-fold or higher in the SERS [8,16], the enhancing effect of SEIRAS varies at most in the range from 10 to 10^3-fold [11,14,15]. For the SERS, the structural effects of AuNPs have been investigated [8], and the AuNPs used in the measurement system have been developed by the simple agglomeration of spherical AuNPs [13] to the non-spherical AuNPs with modified surfaces [13,19,20]. Meanwhile, although the structural effects of NPs for the SEIRAS have been also reported, the research is limited [14,15]. Then, it may be considered that the enhancement in SEIRAS can be improved by the modifications of the structure of AuNPs and their surfaces.

In the present study, a new type of AuNP, confeito-like AuNP [21–23], was used for SEIRAS, and the effects of the confeito-like structure and the surface condition were discussed. Moreover, the SEIRAS was examined with the transmission mode [24–26] instead of the ATR mode [27,28]. The Au film was simply prepared by spreading the non-spherical AuNPs without metal evaporator. This attempt will provide a convenient approach for SEIRAS. Since it has

Abbreviations: AuNP, Au nanoparticles; SERS, surface-enhanced Raman scattering; SEIRAS, surface-enhanced IR absorption spectroscopy; EF, enhancing factor.

* Corresponding author. Tel.: +886 2 2730 3773; fax: +886 2 2730 3733.
E-mail addresses: masaki.ujihara@mail.ntust.edu.tw, masaki.ujihara@gmail.com (M. Ujihara).

http://dx.doi.org/10.1016/j.jtice.2014.06.021
1876-1070/

been reported that the confeito-like AuNPs have strong enhancing effect for the Raman scattering [21,22], the insight for enhancement on IR absorption in the present study will be useful to design the comprehensive devices for both SERS and SEIRAS, which can be handy and allow ultrasensitive analyses.

2. Experimental

2.1. Reagents

Sodium tetrachloroaurate(III) dihydrate ($NaAuCl_4{\cdot}2H_2O$, 99%) was purchased from Sigma–Aldrich Co. (USA). Anhydrous citric acid, sodium hydroxide (NaOH), chloroform, and an aqueous solution of hydrogen peroxide (H_2O_2, 35 wt%) were purchased from Acros Organics (USA). Eicosanoic acid was obtained from Wako Pure Chemical Industries (Japan). All chemicals were of reagent grade and used without further purification. Ultrapure (Millipore Milli-Q) water with a resistivity of 18.2 MΩ cm was used throughout all the syntheses and measurements in the study.

2.2. Synthesis of confeito-like AuNPs

The confeito-like AuNP was synthesized according to the method previously reported [22,23]. Typically, citric acid (31.2 mg) was dissolved in 28 cm^3 of water. Then, 4 cm^3 of an aqueous solution of $NaAuCl_4$ (1 mM) was added into the solution of citric acid. Subsequently, 160 mm^3 of H_2O_2 (35 wt%) was added to the solution. Finally, 8 cm^3 of an aqueous solution of NaOH (100 mM) was mixed with vigorous stirring for 1 min. The reaction solution was allowed to stand overnight for the completion of reaction, and a dispersion of AuNPs was obtained.

2.3. Preparation of gold thin film for SEIRAS

The dispersion of confeito-like AuNP was centrifuged (10,000 rpm, 5590 × *g*, 10 min) and diluted to 1, 5, and 10 mM/Au with water for further experiments. The dispersions of AuNP (20 mm^3) at different concentrations were put on CaF_2 plates (13 mm in diameter) and dried for 1 h to form the films with a diameter of 5 mm. Then, the chloroform solution of eicosanoic acid (6–30 μM, 6 mm^3) was spread on the CaF_2 plates and dried.

2.4. Instruments

Scanning electron microscopic (SEM) images were obtained with a JEOL JSM-6500F microscope. Transmission electron microscopic (TEM) images were taken on a Hitachi H-7000 instrument at an accelerating voltage of 100 kV. For SEM and TEM observations, the specimens were prepared by dropping the dispersion of AuNPs (1 mM, 5 mm^2) on carbon-coated copper grids and air-dried. Ultraviolet-visible-near infrared (UV-vis-NIR) absorption spectra were recorded with a JASCO V-670 spectrophotometer with quartz cells of 10 and 1 mm light paths for the dispersion. Optical microscopic images of AuNPs on CaF_2 were taken using an ECLIPSE TE2000-U microscope (Nikon, Japan). Fourier transform infrared (FT-IR) absorption spectra were acquired with transmission method by using a nicolet-6700 IR spectrometer.

3. Results and discussion

The preparation of confeito-like AuNPs was followed previous reports [22,23]. The structure of obtained confeito-like AuNP was characterized by SEM and TEM (Fig. 1A and B). The particles were around 60–80 nm in diameter and had many bosses on their surfaces. The surface of AuNPs was covered by layers of low

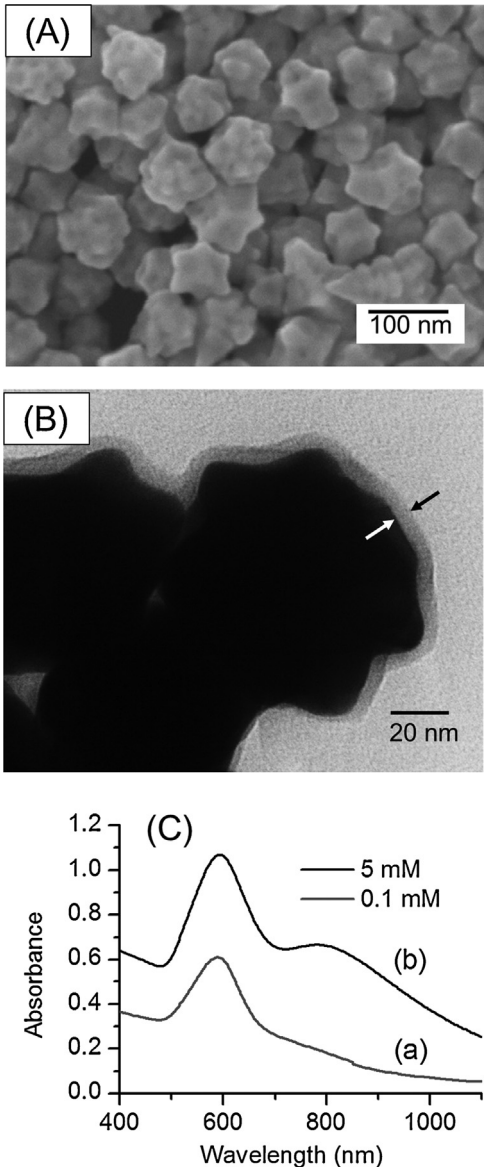

Fig. 1. Characteristics of the confeito-like Aunts. (A) A SEEM image, (B) a TEM image, and (C) UV-vis-NIR absorption spectra of dispersions. Concentration: (a) 5 mM and (b) 0.1 mM. Light path of quartz cell: (a) 1 cm and (b) 1 mm.

electron density with a thickness of several nm (Fig. 1B), and they could be the adsorbed layer of citrate [22,24–29]. The UV-vis-NIR absorption spectrum of the dispersion of confeito-like AuNP (Fig. 1C) indicated that this AuNP had a broad plasmon absorption band at 590 nm, which was much longer than the plasmon absorption band (~550 nm) of spherical AuNPs with corresponding size [2]. This suggests that the morphology of confeito-like AuNPs resulted in the shift of surface-plasmon absorption band [21–23]. After centrifugation, the absorption band at 590 nm was maintained, but a new band appeared around 790 nm (Fig. 1C). This new band could be the plasmon absorption band of the agglomerates of the confeito-like AuNPs [8,9,30], which were formed during the concentration process by centrifugation. When the dispersion of confeito-like AuNP was spread and dried on a CaF_2 substrate, the AuNPs were observed as dark-blue spots (mostly smaller than 1 μm) under an optical microscope (Fig. 2A–C). This suggests that some AuNPs agglomerated and formed island structures on the substrate.

Prior to the measurement of SEIRAS, the films of AuNPs prepared from the dispersions of different concentrations were

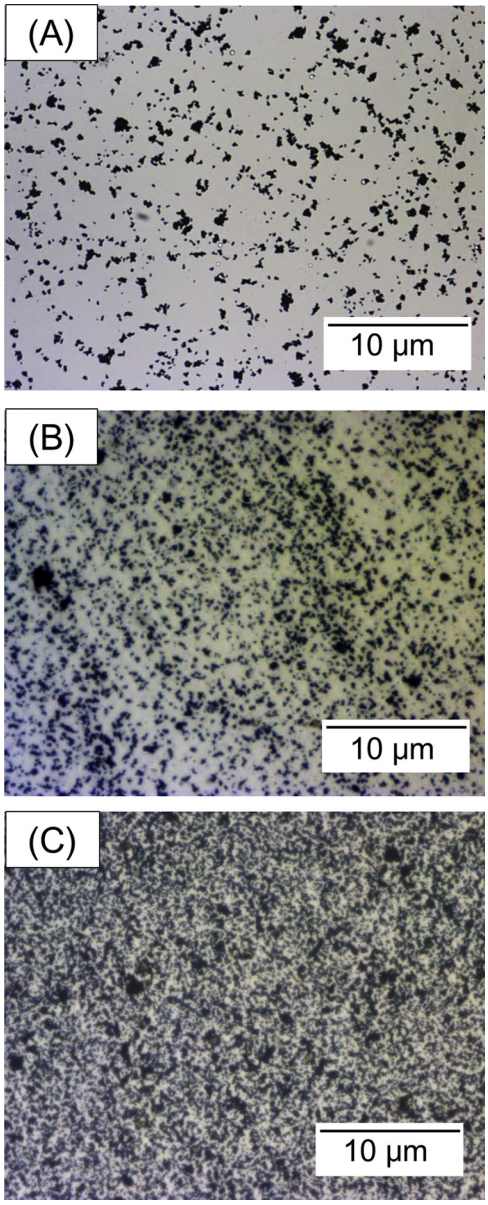

Fig. 2. Optical microscopic images of films on CaF_2 substrates, which were prepared from dispersions of (A) 1 mM, (B) 5 mM, and (C) 10 mM.

characterized by IR absorption spectroscopy (in the supplementary material, Fig. s1). Although the remaining citrate provided several absorption bands, which were assigned to $-COO^-$ groups of citrate (1577 and 1388 cm^{-1}) and –OH groups of adsorbed water (broad band around 3300 cm^{-1}), the bands corresponding to $-CH_2-$ groups were negligibly small. On the other hand, a film of eicosanoic acid, which was prepared by spreading its solution (1 mM, 6 mm^3) on the CaF_2 substrate, had prominent stretching vibration bands of methylene group (antisymmetric: 2918 cm^{-1} and symmetric: 2848 cm^{-1}). Then, the absorption bands for CH_2 stretching vibration modes of eicosanoic acid were used to evaluate the surface-enhancing effect of AuNPs.

For SEIRAS, eicosanoic acid was spread on the films of AuNPs on CaF_2 substrate, and then the IR spectra were measured in comparison with the spectrum from the AuNPs on CaF_2 substrate without the eicosanoic acid. The obtained spectra in the range of 2800–3000 cm^{-1} are shown in Figs. 3 and s2. The enhancing factors (EFs) of SEIRAS were calculated for these antisymmetric and symmetric stretching bands and plotted against the

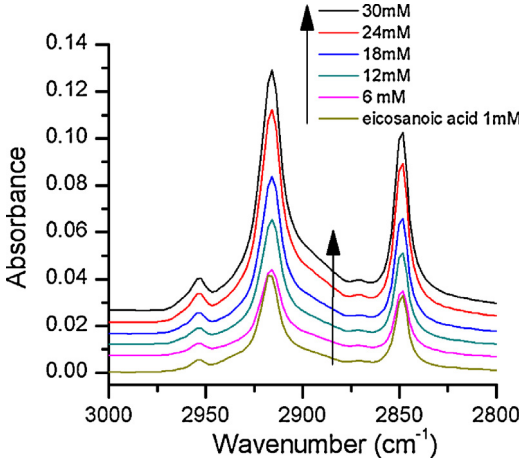

Fig. 3. SIERRAS of eicosanoic acid on films of confeito-like Aunts. The concentration of dispersion of Aunts was 1 mM. Concentrations of eicosanoic acid are indicated in figure.

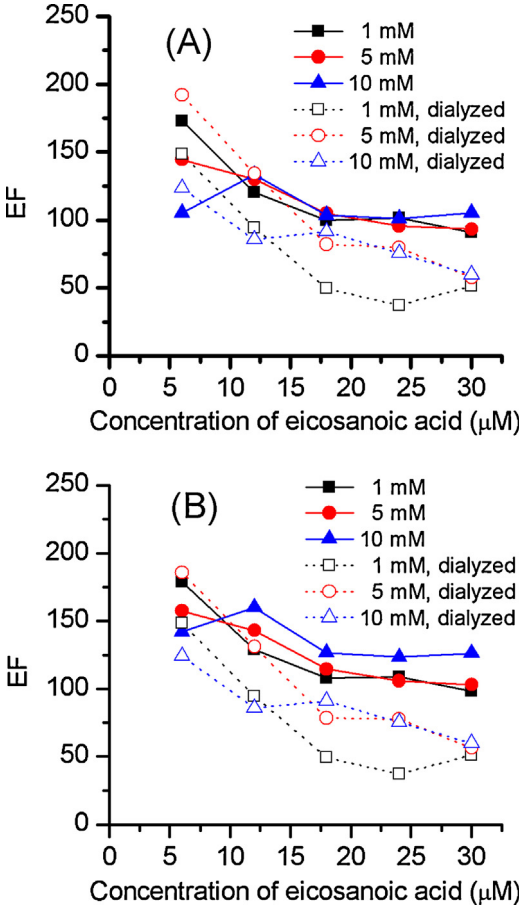

Fig. 4. Plot of enhancing factors as a function of concentration of eicosanoic acid. (A) CH_2 symmetric stretching band and (B) CH_2 antisymmetric stretching band. Concentrations of Aunts and dialyzed Aunts are indicated in figure.

concentration of eicosanoic acid (Fig. 4). The calculation of EFs is based on the following formula [14,15].

$$EF = \left(\frac{A_{SEIRAS}}{A_{Control}}\right) \cdot \left(\frac{C_{Control}}{C_{SEIRAS}}\right) \quad (1)$$

where A_{SEIRAS}: absorbance of enhanced band of eicosanoic acid; $A_{Control}$: absorbance of corresponding band of the control; C_{SEIRAS}: concentration of eicosanoic acid; $C_{Control}$: concentration of the control (1 mM).

The EFs reached up to ~200 and gradually decreased as the amount of eicosanoic acid increased. This decrease can be explained by the distance of target molecules from the surface of AuNP [1–5,11,12] the enhancing effect works only in the vicinity of the AuNPs. Therefore, the distribution of eicosanoic acid, spread on the substrate or accumulated on the AuNPs, is important for the effective SEIRAS. In this study, the spread eicosanoic acid was 6–30 μM × 6.0 mm^3 on a CaF_2 substrate, that is, 0.4–1.8 × 10^{-10} mol. The molecular area of alkyl chain in all-*trans* conformation is ~0.20 nm^2 [31], and then, the eicosanoic acid spread on the substrate would occupy 0.04–0.22 cm^2. This area was around 3–17% of the surface of CaF_2 substrate (1.3 cm^2), if the eicosanoic acid could form a monolayer on the substrate. On the other hand, the amount of confeito-like AuNPs spread on the substrate was (2–20) × 10^{-8} mol (corresponding to the concentration of 1–10 mM/Au), and their total surface areas were estimated to be 0.2–2 cm^2 as spherical particles of 70 nm in diameter (the specific surface area of ~4 m^2/g). Then, the total surface area of AuNPs can be larger than the occupied area of monolayer of eicosanoic acid. The film of eicosanoic acid adsorbed on AuNPs could be thin enough for SEIRAS, and the decreasing of EFs at high concentration of eicosanoic acid could be ascribed to the distribution of eicosanoic acid on the substrate.

The EFs around 200 are rather high in comparison with the EFs already reported (usually 10–100) [11]. This high efficiency suggests that the target molecules were trapped well near the AuNPs [8,13,15–18]. In detail, the EFs were not significantly changed by the amount of AuNPs spread on the substrate (Fig. 4), although the variation of amount of AuNPs was 10 times. This behavior can be explained by the fact that some of AuNPs were embedded in the agglomerates, as seen in Fig. 1, and they could not contribute to the surface-enhancing. For the confeito-like AuNPs, the enhanced electromagnetic fields can be projected from the tips on surface [21–23,32–34], while the hot-sites in the films of spherical AuNPs are formed at the inter-particle junctions [8,13,15]. Then the surface-enhancing effect of confeito-like AuNP does not strongly occur in the agglomerates but occurs mainly at the surface of their film. Similar behaviors were also reported for the SERS using non-spherical AuNPs [19,20,32–34]. This means that the EF of SEIRAS can be improved by changing the film structure to expose confeito-like AuNPs without agglomeration on film surface. The confeito-like AuNPs may have an advantage for the suitable film configuration, because they have basically spherical morphology to face the hot-site toward the outside of the film, while the other nano-structures, such as nano-rods, should be arranged perpendicularly to the substrate for effective surface-enhancing [35].

The only sparsely distributed confeito-like AuNPs indicated the EF around 200 (Fig. 4), and this implies that the net effect of the confeito-like AuNPs may be higher than the observed EFs. Otherwise, the eicosanoic acid is selectively accumulated on the AuNPs. Since citrate molecules cover the surfaces of the confeito-like AuNPs as the adsorbed layer (Fig. 1B) [29], the distribution of eicosanoic acid could be affected by the citrate. To demonstrate the effect of citrate, the confeito-like AuNPs were dialyzed using a cellulose tube (MWCO 1000) and used for SEIRAS measurements. The calculated EFs of dialyzed confeito-like AuNP were plotted in Fig. 4. When the amount of eicosanoic acid was less, the dialyzed AuNPs provided similar EFs to the undialyzed AuNPs. However, the EFs of dialyzed confeito-like AuNPs became lower than that of undialyzed AuNPs as the large amount of eicosanoic acid is supplied. This behavior suggests that the citrate layer on the AuNPs played an important role to maintain the highly concentrated eicosanoic acid at the hot-sites of confeito-like AuNPs.

To confirm the anchoring effect of the citrate, the molecular arrangement of adsorbed eicosanoic acid on the AuNPs was

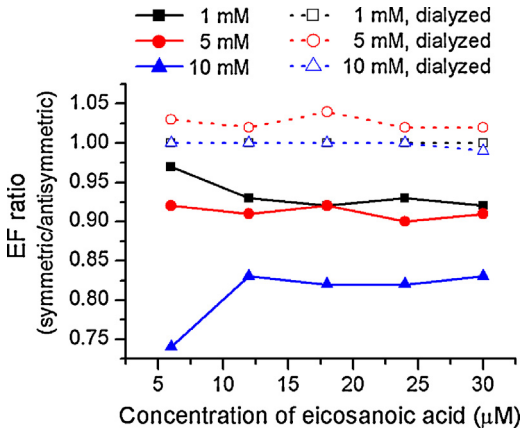

Fig. 5. Plot of ratio of enhancing factors for symmetric and antisymmetric bands as a function of concentration of eicosanoic acid. Concentrations of Aunts and dialyzed Aunts are indicated in figure.

evaluated by the ratios of EFs (symmetric/antisymmetric modes) (Fig. 5). On the AuNPs without dialysis, the symmetric mode was generally less enhanced than the antisymmetric mode in the SEIRAS, and the ratio decreased as the amount of AuNP increased. This anisotropic effect suggested that the molecules of eicosanoic acid took an ordered structure on the AuNP [36], and the abundant amount of AuNP strengthened the orientation of molecules due to the dense coverage of eicosanoic acid on the substrate [37]. On the other hand, the AuNPs after dialysis enhanced equally the two absorption bands. This means that less molecules of eicosanoic acid were adsorbed on the AuNPs with less citrate, and the low density of adsorbed molecules led to the loose packing in the adsorption film. Therefore, the citrate plays an important role to arrange the eicosanoic acid on AuNPs.

The anchoring effect of citrate covering on the surface of AuNP can be caused by the hydrogen bonding of citrate with eicosanoic acid. This anchoring effect and the orientation of alkyl chains are also supported by the shift in band positions of C–H stretching modes in SEIRAS: on the AuNPs covered by citrate, the antisymmetric stretching mode and the symmetric mode of –CH_2– appeared at 2916 cm^{-1} (except the series of 1 mM/Au) and 2850 cm^{-1}, respectively. Meanwhile the eicosanoic acid spread on the CaF_2 substrate indicated the antisymmetric stretching mode and the symmetric stretching mode at 2918 cm^{-1} and 2848 cm^{-1}, respectively. These band positions and their shifts suggest that the alkyl chain of eicosanoic acid on the AuNP took almost all-*trans* conformation, and the crystallinity was even stronger on the AuNP with citrate than in bulk film [36–38]. The SEIRAS on the AuNPs after dialysis had the band positions at 2918 cm^{-1} and 2848 cm^{-1}, which suggested that the orientation of molecules on the AuNPs with less citrate was similar to that in bulk film but weaker than that on the undialyzed AuNPs.

4. Conclusions

The confeito-like AuNPs are the AuNPs with many bosses on the surfaces and have basically spherical structures. In this study, the confeito-like AuNPs with a diameter around 60–80 nm was used for the SEIRAS. Eicosanoic acid was spread on the film of confeito-like AuNP, and then the IR absorption spectra of eicosanoic acid were observed with transmission mode. The IR absorption bands were strongly enhanced at the low amount of the eicosanoic acid. The enhancing factor achieved around 200 and slowly decreased as the amount of eicosanoic acid increased.

This high efficiency of the confeito-like AuNPs for the SEIRAS can be due to the hot-sites on tips on confeito-like AuNP. The

enhanced electromagnetic field was not constrained in the junctions in agglomerates, and then the large amount of eicosanoic acid can be excited on the confeito-like AuNPs than in agglomerates of particles. Comparing with the IR absorption bands of bulk film, the symmetric and antisymmetric stretching bands of $-CH_2-$ in eicosanoic acid on AuNP changed their intensity ratio and band positions. This suggested that citrate covering on the AuNP anchored the eicosanoic acid on the AuNP. This assumption was reinforced by the decreasing of enhancing effect after removal of citrate. The increasing amount of AuNP did not heighten the enhancing factor because of the agglomeration of AuNPs. This suggests that the optimization of film formation would improve the EFs. These findings are useful to design the plasmonics devices for ultrasensitive assay using SEIRAS based on the simple procedure.

Acknowledgments

This work was partly supported by grants of National Science Council of Taiwan (100-2113-M-011-002-MY2) and National Taiwan University of Science and Technology (100B1212).

Appendix A. Supplementary data

Supplementary data associated with this article can be found, in the online version, at http://dx.doi.org/10.1016/j.jtice.2014.06.021.

References

[1] Maier SA, Atwater HA. Plasmonics localization and guiding of electromagnetic energy in metal/dielectric structures. J Appl Phys 2005;98:011101.
[2] Jain PK, Lee KS, El-Sayed IH, El-Sayed MA. Calculated absorption and scattering properties of gold nanoparticles of different size, shape, and composition: applications in biological imaging and biomedicine. J Phys Chem B 2006;110:7238–48.
[3] Murray WA, Barnes WL. Plasmonic materials. Adv Mater 2007;19:3771–82.
[4] Ho FH, Wu YH, Ujihara M, Imae T. A solution-based nano-plasmonic sensing technique by using gold nanorods. Analyst 2012;137:2545–8.
[5] Ghosh SK, Pal T. Interparticle coupling effect on the surface plasmon resonance of gold nanoparticles: from theory to applications. Chem Rev 2007;107:4797–862.
[6] Link S, El-Sayed MA. Spectral properties and relaxation dynamics of surface plasmon electronic oscillations in gold and silver nanodots and nanorods. J Phys Chem B 1999;103:8410–26.
[7] Manna A, Imae T, Aoi K, Okada M, Yogo T. Synthesis of dendrimer-passivated noble metal nanoparticles in a polar medium: comparison of size between silver and gold particles. Chem Mater 2001;13:1674–81.
[8] Xu H, Aizpurua J, Käll M, Apell P. Electromagnetic contributions to single-molecule sensitivity in surface-enhanced Raman scattering. Phys Rev E 2000;62:4318–24.
[9] Tian ZQ, Ren B, Wu DY. Surface-enhanced Raman scattering: from noble to transition metals and from rough surfaces to ordered nanostructures. J Phys Chem B 2002;106:9463–83.
[10] Ataka K, Hara Y, Osawa M. A new approach to electrode kinetics and dynamics by potential modulated Fourier transform infrared spectroscopy. J Electroanal Chem 1999;473:34–42.
[11] Ataka K, Heberle J. Biochemical applications of surface-enhanced infrared absorption spectroscopy. Anal Bioanal Chem 2007;388:47–54.
[12] Metiu H. Surface enhanced spectroscopy. Prog Surf Sci 1984;17:153–320.
[13] Moskovits M. Surface-enhanced Raman spectroscopy: a brief retrospective. J Raman Spectrosc 2005;36:485–96.
[14] Zhang Z, Imae T. Study of surface-enhanced infrared spectroscopy 1. Dependence of the enhancement on thickness of metal island films and structure of chemisorbed molecules. J Colloid Interface Sci 2001;233:99–106.
[15] Zhang Z, Imae T. Study of surface-enhanced infrared spectroscopy 2. Large enhancement achieved through metal–molecule–metal sandwich configurations. J Colloid Interface Sci 2001;233:107–11.
[16] Nedelkovski V, Schwaighofer A, Wraight CA, Nowak C, Naumann RLC. Surface-enhanced infrared absorption spectroscopy (SEIRAS) of light-activated photosynthetic reaction centers from rhodobacter sphaeroides reconstituted in a biomimetic membrane system. J Phys Chem C 2013;117:16357–63.
[17] Gutierrez-Sanz O, Marques M, Pereira IAC, De Lacey AL, Lubitz W, Rüdiger O. Orientation and function of a membrane-bound enzyme monitored by electrochemical surface-enhanced infrared absorption spectroscopy. J Phys Chem Lett 2013;4:2794–8.
[18] Yang YY, Ren J, Li QX, Zhou ZY, Sun SG, Cai WB. Electrocatalysis of ethanol on a Pd electrode in alkaline media: an in situ attenuated total reflection surface-enhanced infrared absorption spectroscopy study. ACS Catal 2014;4:798–803.
[19] Orendorff CJ, Gearheart L, Janaz NR, Murphy CJ. Aspect ratio dependence on surface enhanced Raman scattering using silver and gold nanorod substrates. Phys Chem Chem Phys 2006;8:165–70.
[20] Lu Y, Liu GL, Kim J, Mejia YX, Lee LP. Nanophotonic crescent moon structures with sharp edge for ultrasensitive biomolecular detection by local electromagnetic field enhancement effect. Nano Lett 2005;5:119–24.
[21] Sharma J, Tai Y, Imae T. Synthesis of confeito-like gold nanostructures by a solution phase galvanic reaction. J Phys Chem C 2008;112:17033–37.
[22] Ujihara M, Imae T. Versatile one-pot synthesis of confeito-like Au nanoparticles and their surface-enhanced Raman scattering effect. Colloids Surf A 2013;436:380–5.
[23] Ujihara M, Dang NM, Imae T. Fluorescence quenching of urbanise on confeito-like Au nanoparticles. J Menisci Nanotechnol 2014;14:4906–10.
[24] Ito M, Imae T, Aoi K, Tsutsumiuchi K, Noda H, Okada M. In situ investigation of adlayer formation and adsorption kinetics of amphiphilic surface-block dendrites on solid substrates. Langmuir 2002;18:9757–64.
[25] Yamazaki T, Imae T. Preparation of dendrite SAM on Au substrate and adsorption/adsorption of poly-L-glutamate on the SAM. J Menisci Nanotechnol 2005;5:1066–71.
[26] Ito M, Imae T. Self-assembled monolayer of carboxyl-terminated poly(amide amine) dendrite. J Menisci Nanotechnol 2006;6:1667–72.
[27] Imae T, Takeshita T, Yahagi K. In situ adsorption investigation of hexadecyltrimethylammonium chloride on self-assembled minelayers by surface plasmon resonance and surface enhanced infrared absorption spectroscopy. Stud Surf Sci Catal 2001;132:477–80.
[28] Nagaoka H, Imae T. Poly(amide amine) dendrite adsorption onto 3-mercaptopropionic acid self-assembled monolayer formed on Au surface-investigation by surface enhanced spectroscopy and surface plasmon sensing. Trans Mater Res Soc Jpn 2001;26:945–8.
[29] Kimling J, Maier M, Okenve B, Kotaidis V, Ballot H, Plech A. Turkevich method for gold nanoparticle synthesis revisited. J Phys Chem B 2006;110:15700–07.
[30] Ujihara M, Orbulescu J, Imae T, Leblanc RM. Film structures of poly(amide amine) dendrites with an azacrown core and long alkyl chain spacers on water or Ag nanoparticle suspension. Langmuir 2005;21:6846–54.
[31] Ujihara M, Imae T. Adsorption behaviors of poly(amide amine) dendrites with an azacrown core and long alkyl chain spacers on solid substrates. J Colloid Interface Sci 2006;293:333–41.
[32] Hao E, Bailey RC, Schatz GC, Hupp JT, Li S. Synthesis and optical properties of branched gold nanocrystals. Nano Lett 2004;4:327–30.
[33] Khoury CG, Vo-Dinh T. Gold Nan stars for surface-enhanced Raman scattering: synthesis, characterization and optimization. J Phys Chem C 2008;112:18849–59.
[34] Jeong GH, Lee YW, Kim M, Han SW. High-yield synthesis of multi-branched gold nanoparticles and their surface-enhanced Raman scattering properties. J Colloid Interface Sci 2009;329:97–102.
[35] Zhang X, Imae T. Perpendicular superlattice growth of hydrophobic gold nanorods on patterned silicon substrates via evaporation-induced self-assembling. J Phys Chem C 2009;113:5947–51.
[36] Myrzakozha DA, Hasegawa T, Nishijo J, Imae T, Ozaki Y. An infrared study of molecular orientation and structure in one-layer Langmuir–Boldest films of octadecyldimethylamine oxide and dioctadecyldimethylammonium chloride: dependence of the structures of the Langmuir–Boldest films on substrates, aging, and pH of water subphase. Langmuir 1999;15:6890–6.
[37] Myrzakozha DA, Hasegawa T, Nishijo J, Imae T, Ozaki Y. Structural characterization of Langmuir–Boldest films of octadecyldimethylamine oxide and dioctadecyldimethylammonium chloride. 2. Thickness dependence of thermal behavior investigated by infrared spectroscopy and wetting measurements. Langmuir 1999;15:3601–7.
[38] Niidome Y, Hisanabe H, Hori A, Yamada S. Surface enhanced IR absorption spectroscopy of dodecanethiol monolayer adsorbed on the laser-deposited gold nanoparticles. Anal Sci 2001;17:i1185–88.